Calculated properties of field-induced aggregates in ferrofluids

F. Marty Ytreberg and Susan R. McKay
Department of Physics and Astronomy, University of Maine, Orono, Maine 04469-5709
(Received 27 September 1999)

We have calculated the critical radius of aggregates in thin layers of ferrofluid, assuming a cylindrical aggregate shape, as a function of external field and plate separation. Results are obtained by minimizing the Helmholtz free energy, and can be used to predict aggregate radius and spacing. The model, with entropy included, provides reasonable predictions for the onset of the labyrinth pattern. These results show good agreement when compared with data from experiments on Fe_3O_4 kerosene-based ferrofluids and magnetorheological fluids.

PACS number(s): 77.84.Nh, 47.54.+r, 47.65.+a

I. INTRODUCTION

Ferrofluids, or magnetic colloids, pose interesting questions for both scientists and engineers. For the physicist, there are many new fundamental hydrodynamic, and physical problems that arise when a ferrofluid is exposed to a magnetic field [1–6]. For engineers, the ferrofluid's ability to undergo a phase transition from liquid to solid in the presence of a magnetic field makes it useful for practical applications such as magnetofluidic seals, dampers, magnetic drug delivery, and many others [7–10].

Ferrofluids are composed of very small one-domain paramagnetic particles dispersed in a carrier, such as kerosene [1]. The particles are small enough, around 10 nm in diameter, that Brownian motion keeps them randomly dispersed throughout the carrier in the absence of a magnetic field, and they are coated with a surfactant to prevent clumping due to van der Waals forces. Thus the particle-particle interactions are restricted to a steric repulsion due to the surfactant and a dipole-dipole interaction [3].

In the experiment of interest to us, the ferrofluid is confined between two glass plates with a separation L, and then an external magnetic field H_0 is applied normal to the plates. On the order of 10 s after the field is applied, the particles form single particle diameter chains and, on the order of 10^4 s later, the chains clump together to form aggregates [4]. A view normal to the glass plates shows two-dimensional patterns such as hexagonal and labyrinth. The focus of this paper is to predict the size and spacing of the aggregates for a hexagonal pattern, once equilibrium has been reached, as a function of H_0 and L. We compare our theory to the experiments done by Hong *et al.* [4], Horng *et al.* [6], Liu *et al.* [2], Flores and co-workers [9,11], Wang *et al.* [5], and Bacri and co-workers [12,13], using approximately 10 nm Fe_3O_4 particles in kerosene. The theory is then used to predict the onset of a structural phase transition as a function of H_0 and L.

II. HELMHOLTZ FREE ENERGY

Since it is reasonable to say that the time scale associated with changes in the shape of an aggregate is small compared to the time scale associated with the formation of an aggregate from the chains, we treat the formation of the aggregates as a quasiequilibrium process. Thus, in accordance with references such as Refs. [2,3,12,14], the size of an aggregate can be determined by a minimization of the free energy. Assuming cylindrically shaped aggregates that span the thickness of the container, a close approximation to experimental observations, the problem is reduced to finding the energetically favorable aggregate radius b.

Our model differs from those previously studied (such as Refs. [2,3,5,12,14]) in that it includes an entropy term. The addition of this configurational entropy proves important in determining the equilibrium state of the system at typical experimental temperatures ($\sim$300 K), shifting the predicted aggregate radii to smaller values. Further, the inclusion of entropy changes the range of external field and plate separation for which the hexagonal array of aggregates is stable, providing good qualitative agreement with experimentally observed trends. Since the diameter of the aggregates is on the order of several microns, the entropy associated with Brownian motion is not included (see also Ref. [5]).

The long-range attraction between chains, responsible for the aggregation, is not well understood [2,15,16]. Martin *et al.* [17] proposed that the Landau-Peierls thermal instability could be responsible for this attraction in electrorheological fluids. However, it is not clear that this explanation can be extended to ferrofluids. Gross and Kiskamp [15] introduced a new long range attraction for two chains of dipoles, but their result is only valid at absolute zero temperature. The theory in this paper assumes that the chains will clump together and asks, under this assumption, what will be the energetically favorable aggregate size. As developed below, the model is not sensitive to the details of the attractive chain-chain interaction.

A. Magnetic energy

In calculating the magnetic energy of the system, there are two interactions that must be taken into account. One is the interaction between an aggregate and each of its neighboring aggregates, and the other includes the interaction of the aggregates with the external magnetic field.

The interaction energy between an aggregate and its neighbors can be calculated in accordance with Liu *et al.* [2]. In this model the ends of the aggregates are thought of as disks of uniformly distributed monopoles. There are two terms to consider; the first is the repulsion between disks in the same plane, and the second term is the attraction between

disks in opposite planes. The resulting magnetic energy of the system (compare with Ref. [2]) can be written as

$$E_{MTot} = \xi_1 M^2 b - \xi_2 M^2 \frac{b^2}{L}. \quad (1)$$

Here, ξ_1 and ξ_2 are constants which depend upon the properties of the aggregate, M is the constant magnetization of an aggregate, and we have used the fact that the aggregate radius is directly proportional to the aggregate spacing (i.e., $b \propto d$, see the Appendix). We add an important assumption, that the magnetization of an aggregate is directly proportional to the external field strength. When the external field is turned on (i.e., not ramped slowly), the particles do not have time to align with the field before becoming part of a chain. Thus the magnetization of a chain, and therefore an aggregate, is determined by the amount of average alignment obtained by the particle. The larger the field, the more a particle will be able to align before chaining, and thus the higher the magnetization. It is reasonable to think that, on average, the particles are aligned with the external field, thus the magnetization is parallel to the external field. With these assumptions, our model is expected to work best with low to moderate field strengths. Now this part of the magnetic energy of the system becomes

$$E_{MTot} = \eta_1 H_0^2 b - \eta_2 H_0^2 \frac{b^2}{L}. \quad (2)$$

To calculate the interaction energy of the aggregates with the external magnetic field, we approximate the aggregates as dipoles. This approximation is reasonable since $b \ll d$ for the low volume fractions under consideration here. The energy of this interaction is $-\vec{m} \cdot \vec{H_0}$, where $\vec{m}$ is the magnetic moment of the aggregate. Using the assumption above that all of the magnetic particles within the aggregate are, on average, aligned with the field, we can write $\vec{m} = (\pi b^2 L)\vec{M}$. To calculate the total interaction energy we must multiply this single aggregate energy by the total number of aggregates (see the Appendix). Thus this part of the magnetic energy is

$$E_{H_0} = -\frac{\Phi l^2}{\gamma} M H_0 L. \quad (3)$$

Here Φ is the volume fraction of the ferrofluid, γ is the packing fraction of the particles within an aggregate, and the glass plates have area l^2. This contribution to the energy has no b dependence, and thus can be ignored in the minimization process. Therefore the total magnetic interaction energy for the system is given by Eq. (2).

B. Entropy

To calculate the entropy we treat the aggregates as distinguishable. The number of aggregates, N_0, can be determined as a function of aggregate radius (see the Appendix). Therefore, the number of states accessible to the system is $N_0!$, and the configurational entropy of the system is

$$S = k_B \ln(N_0!) = k_B \ln\left(\frac{\Phi l^2}{\gamma \pi b^2}!\right). \quad (4)$$

Using Stirling's approximation, we arrive at the final expression for the entropy:

$$S = k_B \frac{\eta_4}{b^2}\left[\ln\left(\frac{\eta_4}{b^2}\right) - 1\right], \quad \eta_4 = \frac{\Phi l^2}{\gamma \pi}. \quad (5)$$

C. Surface Energy

Several ways of including the surface energy appear in the literature. Halsey and Toor [14] used a surface energy that depends upon the square of the external electric field by applying the Ewald technique to electrorheological fluids. Liu *et al.* [2] used this same form of the surface energy for magnetorheological fluids. According to experimental data produced by Sudo *et al.* [8], the surface tension goes as $H_0^{4/5}$. We choose the simple approach introduced by Zubarev and Ivanov [3], which assumes that the surface tension, σ, is independent of H_0, and depends only upon the two substances present at the interface.

Since we have assumed a cylindrical aggregate shape, we must introduce two surface tension terms: one for the top and bottom of the aggregate, and the other for the sides. The surface energy for a single aggregate is then

$$E_S = \int_S \sigma dS = 2\sigma_1(\pi b^2) + \sigma_2(2\pi b L), \quad (6)$$

where σ_1 and σ_2 are the surface tension for the aggregate-glass and the aggregate-fluid interfaces, respectively.

The total surface energy is the product of the surface energy of a single aggregate and the total number of aggregates, N_0, so

$$E_{STot} = \frac{\Phi l^2}{\gamma \pi b^2} E_S = \frac{2\Phi l^2}{\gamma}\left(\sigma_1 + \sigma_2 \frac{L}{b}\right). \quad (7)$$

Of course, only the second term contributes to finding the aggregate radius that minimizes the free energy. Thus the first term can be ignored in the minimization process. The final surface contribution for use in our minimization of the free energy is then

$$E_{STot} = \eta_3 \frac{L}{b}, \quad \eta_3 = \frac{2\Phi l^2}{\gamma}\sigma_2. \quad (8)$$

III. RESULTS

The Helmholtz free energy formed by combining Eqs. (2), (5), and (8) is

$$F = E_{MTot} + E_{STot} - TS = \eta_1 H_0^2 b - \eta_2 H_0^2 \frac{b^2}{L} + \eta_3 \frac{L}{b} - k_B T \frac{\eta_4}{b^2}\left[\ln\left(\frac{\eta_4}{b^2}\right) - 1\right]. \quad (9)$$

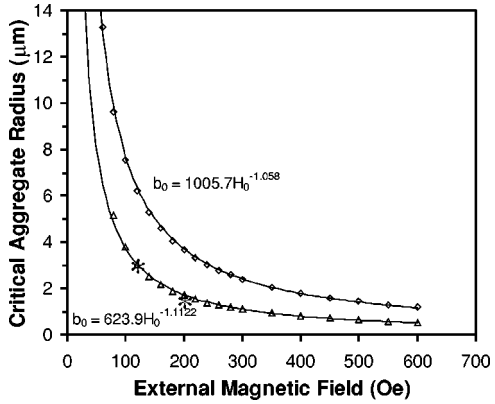

FIG. 1. Critical aggregate radius as a function of external magnetic field. The upper curve (diamonds) is for $L=50.0$ μm, and the lower curve (triangles) is for $L=10.0$ μm. The solid curves represent a power law fit to the numerical results.

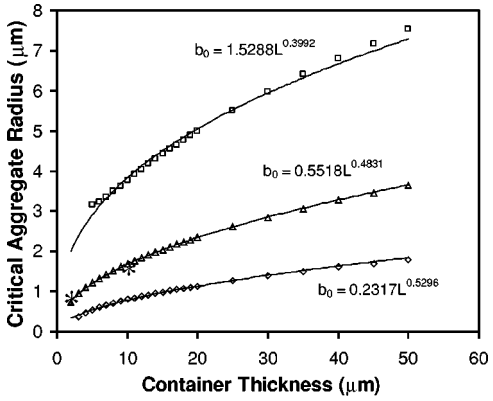

FIG. 2. Critical aggregate radius as a function of container thickness. The upper curve (squares) is for $H_0=100.0$ Oe, the middle curve (triangles) is for $H_0=200.0$ Oe, and the lower curve (diamonds) is for $H_0=400.0$ Oe. The solid curves represent a power law fit of the mathematical data.

Since the expression is too complicated to find the zeros of the first derivative analytically, minima were located numerically.

For all of the plots shown, the values of the constants are $\eta_1=2.0\times10^{-5}$ erg/Oe^{2}cm, $\eta_2=8.0\times10^{-6}$ erg/Oe^{2}cm, $\eta_4=0.05$ cm^2 (which corresponds to $\Phi=0.10$, $l^2=1.0$ cm^2, and $\gamma\approx0.638$, the packing fraction for randomly placed spheres), $\eta_3=2.0\times10^{-5}$ erg (which corresponds to a surface tension of approximately 6.4×10^{-5} erg/cm^2), and finally $T=300.0$ K.

A plot of the energetically favorable radius of the aggregates as a function of external magnetic field, H_0, is shown in Fig. 1. Here the container thickness is fixed at $L=10.0$ μm for the lower curve and $L=50.0$ μm for the upper curve. The data points were obtained from the minima of the free energy, and the solid lines were obtained by a power law fit of the results. The equation corresponding to the power law fit is also included in the figure. The stars are experimental data points obtained from Ref. [4]. Also included in this reference is a graph of aggregate separation as a function of external magnetic field that is in good qualitative agreement with our model. In Ref. [6], Horng *et al.* determined that aggregate spacing goes roughly as the inverse of the applied field. The exponents predicted in our model vary from 1.0 to 1.7, increasing as the layer thickness decreases. Finally, in Refs. [12,13], it was found that increasing the magnetic field led to a decrease in the size of the aggregates, consistent with our results.

Figure 2 is a plot of the energetically favorable radius as a function of L for a fixed external magnetic field of $H_0=100.0$ Oe for the upper curve, $H_0=200.0$ Oe for the middle curve, and $H_0=400.0$ Oe for the lower curve. Once again the data points were obtained from the minima of the free energy, and the solid lines represent a power law fit of the data. The stars on this graph are obtained from Ref. [4]. The exponents are displayed on the figure and can be compared with other models. Previous models, such as Ref. [5], have an exponent that varies from 0.5 for $L<10.0$ μm to 0.67 for thicker layers. This was done for $H_0=300$ Oe. The model, introduced by Liu *et al.* [2], obtained an exponent of 0.37 for magnetorheological fluids with $H_0=380$ Oe. Our model predicts that the exponent will vary from about 0.3 to 0.6, increasing as H_0 is increased.

An interesting feature of this model appears in the loss of the local minimum in the free energy, Eq. (9), as a function of b, for certain regions of parameter space. Shown in Fig. 3 is the phase diagram predicted by this model. The shaded area of the graph is the region of parameter space where the free energy has a well defined local minimum, as a function of b, for finite, nonzero b. This is the region of parameter space where we can expect to make reasonable predictions for aggregate size and spacing for a hexagonal pattern. The other area of the graph is the region of parameter space where there is no local minimum in the free energy for finite b. Thus an ordered hexagonal pattern will not be found, and other patterns could be expected. Since labyrinth patterns have been observed experimentally (see, for example, Refs. [4,5,13]), it is reasonable to think that this region of space will correspond to labyrinth patterns. In Ref. [5], it was

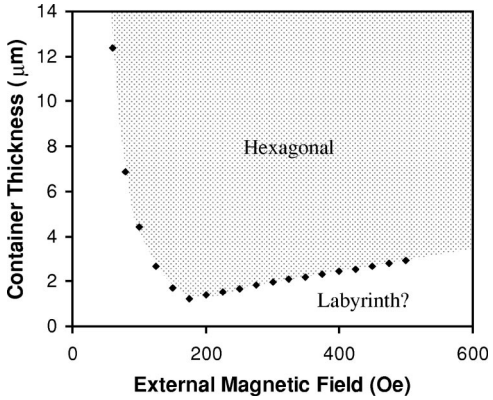

FIG. 3. Phase diagram predicted by model. The shaded area of the graph is the region of parameter space where there is a minimum in the free energy as a function of aggregate radius, b. This is the region of parameter space where we can expect to make reasonable predictions for aggregate size and spacing for a hexagonal pattern. In the other area of the graph, there is no minimum in the free energy as a function of aggregate radius. Thus we expect no hexagonal pattern to form in this region. Instead, other patterns such as labyrinth or disordered phases may form.

found that increasing the thickness of the layer led to a labyrinth pattern. Our model does not predict this behavior, but does predict the behavior seen in Ref. [4]. In Ref. [4], it was found that for small L (2.0 μm), an increase in external field from 200.0 to 400.0 Oe led to a transition from a hexagonal pattern to a labyrinth pattern. This behavior is correctly predicted by our model. In addition, our model indicates that, for low field, an increase in the field leads to a transition from a labyrinth to a hexagonal pattern, which agrees with Ref. [13].

IV. CONCLUSIONS

We have shown that aggregate size and spacing can be qualitatively determined by minimization of the Helmholtz free energy for the ferrofluid system described in Sec. I. This approach differs from others in that it includes the effects of entropy. Previous similar models (such as Refs. [2,5]) predict the aggregate spacing as a function of container thickness only. Our model can also predict trends as a function of external magnetic field strength, in agreement with experiment.

Another feature of this model is the prediction of a structural phase transition, corresponding to the loss of the local minimum in the Helmholtz free energy as a function of aggregate radius. This prediction emphasizes the value of experimental study of the complete phase diagram in the space of external field and plate separation. With these experimental data, the model could be adapted to allow for different forms of the surface energy or alternate aggregate shapes, as discussed in Refs. [3,12,14]. Thus this model captures the features reported for patterns formed in thin ferrofluid layers, and provides a starting point for the development of more detailed, quantitative treatments of complex magnetic fluids.

APPENDIX

Assume that the average radius of N_0 cylindrical aggregates is b, and that the particles lie in the aggregates with a packing fraction γ. Then $N_0\gamma(\pi b^2 L)=\Phi l^2 L$, where L and l are the thickness and length of the container, respectively, and Φ is the volume fraction of the ferrofluid. The number of aggregates as a function of the radius of the aggregate is then

$$N_0=\frac{\Phi l^2}{\gamma\pi b^2}. \tag{A1}$$

For a hexagonal pattern with a spacing, d, between aggregates, it is easy to show that

$$N_0=\frac{2l^2}{d^2\sqrt{3}}. \tag{A2}$$

Using Eq. (A1) above, we find that the spacing between columns as a function of aggregate radius is

$$d=b\sqrt{\frac{2\pi\gamma}{\Phi\sqrt{3}}}. \tag{A3}$$

Thus we see that a plot of b or d, as a function of H_0 or L for fixed volume fraction, differs only by a multiplicative constant.

[1] R. E. Rosensweig, *Ferrohydrodynamics* (Cambridge University Press, New York, 1985).

[2] J. Liu, E. M. Lawrence, A. Wu, M. L. Ivey, G. A. Flores, K. Javier, J. Bibette, and J. Richard, Phys. Rev. Lett. **74**, 2828 (1995).

[3] A. Y. Zubarev and A. O. Ivanov, Phys. Rev. E **55**, 7192 (1997).

[4] C.-Y. Hong, I. J. Jang, H. E. Horng, C. J. Hsu, Y. D. Yao, and H. C. Yang, J. Appl. Phys. **81**, 4275 (1997).

[5] H. Wang, Y. Zhu, C. Boyd, W. Luo, A. Cebers, and R. E. Rosensweig, Phys. Rev. Lett. **72**, 1929 (1994).

[6] H.-E. Horng, C.-Y. Hong, W. B. Yeung, and H.-C. Yang, Appl. Opt. **37**, 2674 (1998).

[7] E. Blums, A. Cebers, and M. M. Mairorov, *Magnetic Fluids* (Walter de Gruyter & Co., Berlin, 1996).

[8] S. Sudo, J. Hashimoto, and A. Ikeda, JSME Int. J. **32**, 47 (1989).

[9] G. A. Flores, J. Liu, M. Mohebi, and N. Jamasbi, Phys. Rev. E **59**, 751 (1999).

[10] C.-Y. Hong, H. E. Horng, I. J. Jang, J. M. Wu, S. L. Lee, W. B. Yeung, and H. C. Yang, J. Appl. Phys. **83**, 6771 (1998).

[11] G. A. Flores, M. L. Ivey, J. Liu, M. Mohebi, and N. Jamasbi, Int. J. Mod. Phys. B **10**, 3283 (1996).

[12] J.-C. Bacri and D. Salin, J. Phys. (France) Lett. **43**, L179 (1982).

[13] J.-C. Bacri, R. Perzynski, and D. Salin, Magn. Liquids (Fr). Recherche **18**, 1150 (1987).

[14] T. C. Halsey and W. Toor, Phys. Rev. Lett. **65**, 2820 (1990).

[15] M. Gross and S. Kiskamp, Phys. Rev. Lett. **79**, 2566 (1997).

[16] E. M. Furst and A. P. Gast, Phys. Rev. E **58**, 3372 (1998).

[17] J. E. Martin, J. Odinek, T. C. Halsey, and R. Kamien, Phys. Rev. E **57**, 756 (1998).